Sensitivity of Parameters Affecting Seismic Risk

Biswajit Dasgupta,[1)] Mahendra Shah,[2)] and Asadul Chowdhury[1)]

1) Center for Nuclear Waste Regulatory Analyses, San Antonio, TX
2) U.S. Nuclear Regulatory Commission, Rockville, MD

ABSTRACT

The Code of Federal Regulations, Title 10, Part 63 (10 CFR Part 63) for the proposed high-level nuclear waste disposal facility at Yucca Mountain, Nevada, USA, is risk-informed and performance-based. The regulations require demonstration of compliance with dose performance objectives for potential risk from natural hazards (e.g., earthquakes). Seismic risk can be evaluated by considering the ability of the structures, systems, and components (SSCs) that are relied on to prevent or mitigate seismically induced event sequences, to perform during a seismic event. Seismic risk or the mean probability of unacceptable performance of an SSC important to safety (ITS), is estimated by convolving the mean seismic hazard (i.e., mean annual probability of exceedance of ground motion level) and the SSC ITS mean fragility (i.e., the mean conditional probability of failure, given the ground motion level) curve. The seismic hazard curves at different sites can have substantially different characteristics (e.g., slopes). The mean fragility curve of an SSC for a defined failure mode or a specified limit state condition is typically defined as being lognormally distributed and can be expressed in terms of a median capacity level, and a composite log standard deviation. The seismic risk computations can be performed either by numerical integration or by a closed-form solution. This study aims at gaining insight on sensitivity of parameters that may affect the seismic risk of SSCs ITS. Effects of the following parameters on the seismic risk are discussed in this paper: (a) discretization steps in the numerical integration method; (b) low probability range of the seismic hazard curve; (b) slope of the hazard curve; and (d) log standard deviation of the fragility curve.

INTRODUCTION

The risk-informed performance-based Code of Federal Regulations, Title 10, Part 63 (10 CFR Part 63) [1], for the proposed geologic high-level nuclear waste disposal facility at Yucca Mountain, Nevada, USA, requires demonstration of compliance with dose performance objectives for potential risk from natural hazards (e.g., earthquakes). The regulations require the applicant to perform preclosure safety analysis for the period before the permanent closure of the facility and demonstrate that structures, systems, and components (SSCs) that are relied on to prevent or mitigate seismically induced event sequences will perform their intended safety functions. A seismic event sequence includes consideration of potential seismically induced initiating events and conditional failure of one or more of these SSCs. For compliance with the regulation, either the probability of occurrence of seismic event sequences, or the estimated radiological dose should be less than the regulatory limit. This paper discusses evaluation of the risk resulting from unacceptable performance of a single such SSC in a seismically initiated event sequence.

Seismic risk, defined here as mean probability of unacceptable performance of an SSC ITS, is estimated by convolving the mean seismic hazard curve with the SSC ITS mean fragility curve [2]. The mean fragility curve for an SSC important to safety (ITS) may be estimated using: (1) probability density functions for controlling parameters in a Monte Carlo analysis; (2) the simplified methods outlined in Section 4 of the Electric Power Research Institute report [3]; or (3) other methods that capture the appropriate variability and uncertainty in parameters used to estimate the capacity of the SSCs ITS to withstand seismic events [4].

The hazard curve and the fragility curve are convolved either by numerical integration or by a closed-form solution. This paper discusses the methodology for evaluating the probability of unacceptable performance and presents the results of the study performed to evaluate the sensitivity of various parameters that could affect the probability of unacceptable performance of SSCs. Effects of the following parameters on the probability of unacceptable performance of an SSC were studied: (a) discretization steps in the numerical integration method; (b) low probability range of the seismic hazard curve; (c) slope of the hazard curve; and (d) log standard deviation of the fragility curve. The purpose of this study is to understand the sensitivity of parameters on the probability of unacceptable performance of SSCs ITS, for regulatory assessment of seismically induced event sequences, and determination of compliance with preclosure safety requirements.

PERFORMANCE EVALUATION METHDOLOGY

A seismic hazard curve, *H(a),* is defined as the mean annual frequency of exceeding a ground motion level, *a*. In this discussion, the ground motion is expressed as spectral acceleration (SA) at a specified natural frequency and damping.

The fragility curve of an SSC, $P_{f|a}$, is the conditional cumulative probability of unacceptable performance (i.e., loss of safety function for a defined failure mode or a specified limit state at a given ground motion level, a). The fragility can be expressed by two parameters: median capacity level, $C_{50\%}$,, and a composite logarithmic standard deviation, β. The mean annual probability of unacceptable performance, P_F, is estimated by convolving the mean seismic hazard, $H(a)$, and the mean fragility, $P_{f|a}$, curves, using Eq. 1. [2, 5, 6]:

$$P_F = \int_0^\infty P_{f|a} \left(-\frac{dH(a)}{da} \right) da, \tag{1a}$$

or

$$P_F = \int_0^\infty H(a) \left(\frac{dP_{f|a}}{da} \right) da \tag{1b}$$

The convolution can be performed by a closed-form solution method or by numerical integration, as discussed below:

Closed-Form Solution Method

The seismic hazard curve is assumed to be linear when plotted in log-log scale and approximated by a power law as [2, 5]:

$$H(a) = K_1 a^{-K_H} \tag{2}$$

Where K_H is the slope parameter given by $K_H = 1/\log(A_R)$, A_R is the ratio of the spectral acceleration (SA), corresponding to tenfold reduction in exceedance probability (i.e., $A_R = SA_{0.1H(a)}/SA_{H(a)}$), and K_1 is a constant obtained using Eq. 3 after K_H is computed.

Approximating the hazard curve by Eq. 2 and considering the fragility to be lognormally distributed with parameters median capacity, $C_{50\%}$,, and log standard deviation, β, the closed-form expression for annual probability of failure of the SSC is given as [6, 7]:

$$P_F = K_1 (C_{50\%})^{-K_H} e^{0.5(K_H \beta)^2} \tag{3}$$

Numerical Integration

For numerical integration, the hazard curve is discretized into equal intervals and assumed to be piecewise linear. The seismic performance is obtained from the product of the hazard exceedance interval, and the fragility value corresponding to the acceleration for each interval, and summed over the entire hazard curve [8].

SEISMIC RISK COMPUTATION

This section presents the data for hazard and fragility curves used in this paper, and discusses the evaluation of seismic risk using either a closed-form solution method, or numerical integration. The hazard curve, shown in Figure 1, was used in this analysis and is based on the data obtained from the U.S. Geological Survey's (USGS's) website for a region in the Western U.S. [9]. The hazard data corresponds to a spectral acceleration of 10 Hertz (Hz). The data from the website were interpolated by statistical line-trend techniques to obtain hazard exceedance probability at tenfold interval from 10E-3 to 10E-7. Maintaining a constant slope between 10E-6 and 10E-7 probability of exceedance, the hazard curve was extrapolated to 10E-9. The hazard curve information obtained from the USGS website is for a firm-rock site condition, and does not include seismic ground response considering overlying soil strata, at any particular site.

Fragility information was obtained from the published survey of data from probabilistic risk analysis studies for nuclear power plants [10]. Fragility information for Heating, Ventilation, and Air Conditioning (HVAC) systems was used as generic data for a representative SSC, in this analysis. Typical failure modes were failure of fan, support, anchor bolts, and base plate. The median fragility range is given as 2.24g–6.9g spectral acceleration, where g is the acceleration of gravity. The database does not include information on the structural frequencies and damping associated with spectral accelerations. The range for random variability, β_r, is estimated as 0.20–0.40, and epistemic uncertainty, β_u, is estimated as 0.24–0.62 [10].

The mean values of β_r and β_u are 0.3 and 0.44, respectively, whereas the mean value of composite logarithmic standard deviation, β, defined as $\sqrt{(\beta_r^2 + \beta_u^2)}$, is 0.53.

Fragility parameters selected in this study were based on the above information. The median fragility or the capacity of an SSC ITS was assumed to be 3.0g spectral acceleration at 10-Hz structural frequency. The range for composite log standard deviation, β, was computed to be 0.31–0.74, based on the extreme ranges of β_r and β_u. However, a range of β was extended from 0.3–0.8 for the purpose of the parametric study.

A mean fragility curve for $C_{50\%}$ = 3.0g and β = 0.4, shown in Figure 2, is used as a baseline case for all parametric studies. The probability of unacceptable performance, P_F, calculated by the closed-form solution method, is 3.4E-5, and by the numerical integration, is 2.26E-5. For the closed-form solution method, the slope between 1.0E-4 and 1.0E-5 probability of exceedance values in the seismic hazard curve was considered, rendering $A_R \approx 1.6$. The difference in the estimated P_F values for the numerical integration and the closed-form expression results from the approximations made in the seismic hazard curve. In the numerical integration, the actual shape of the hazard curve was considered in a finite range, whereas in the closed-form solution, the integration hazard curve is assumed to be a straight line in a log-log scale over the infinite range. The contribution of hazards, in a numerical integration solution to the overall seismic risk, is studied next. ΔP_F from each discretized segment of the hazard curve is normalized by P_F. The histogram of the normalized ΔP_F and the cumulative distribution is plotted with respect to annual spectral acceleration, as shown in Figure 3. It can be seen from Figure 3 that spectral accelerations in the range of 1.2g to 2.7g contribute approximately 80 percent of P_F. This corresponds to the annual probability of exceedance from the hazard curve (Figure 1) approximately between 1.0E-4 and 1.0E-5, and the probability of failure approximately between (Figure 2) 0.01 to 0.4.

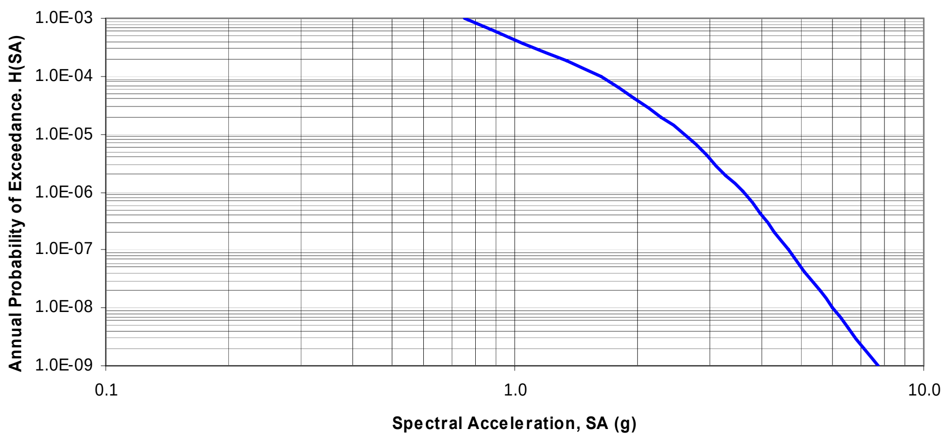

Figure 1: Seismic Hazard Curve for Spectral acceleration at 10 Hz

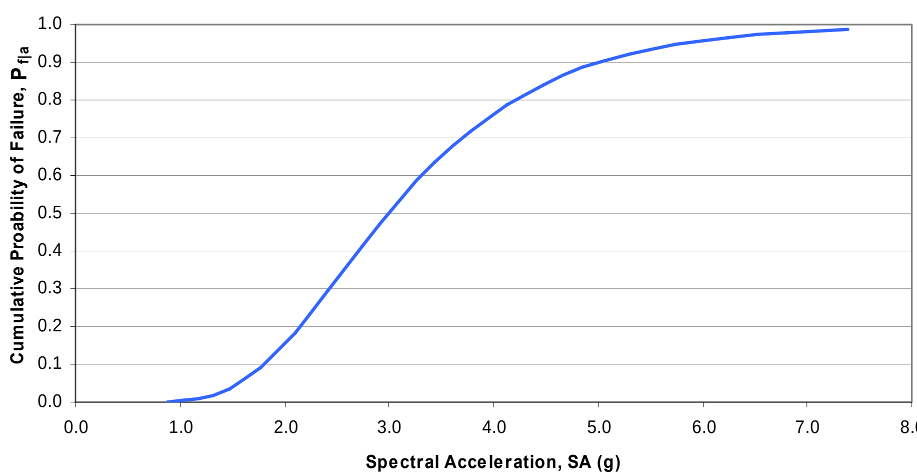

Figure 2: Fragility Curve with $C_{50\%}$ = 3.0 g and β = 0.4 for spectral acceleration at 10 Hz

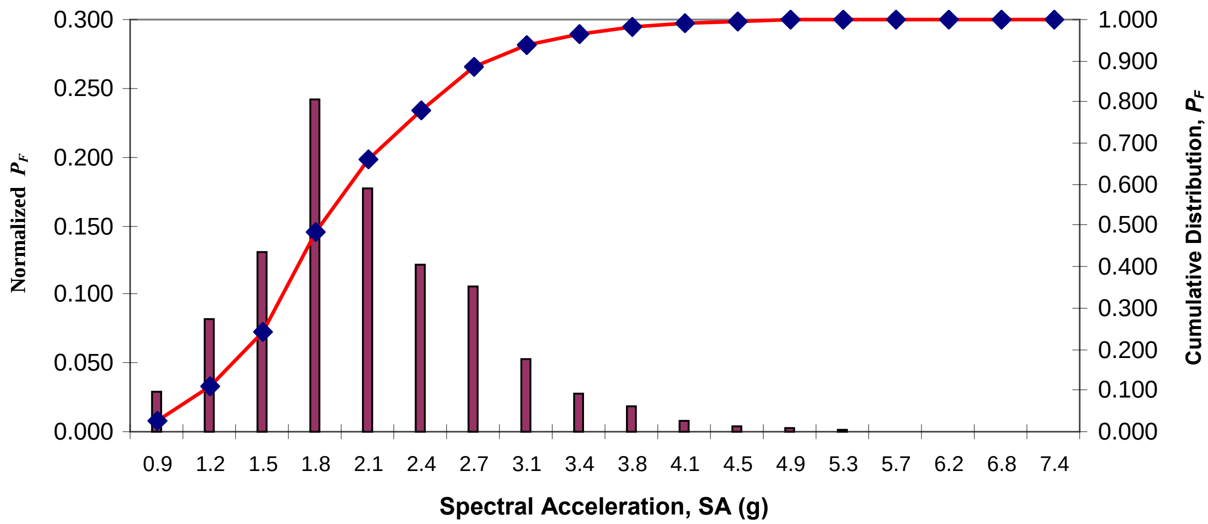

Figure 3: Histogram and Cumulative distribution of P_F vs. Spectral Acceleration

PARAMETRIC STUDY

This study is aimed at evaluating seismic risk, considering unacceptable performance of SSCs ITS, in a preclosure safety analysis. Selected parameters were studied to understand the sensitivity of these parameters on calculation of the probability of unacceptable performance of an SSC. Effects of parameters studied were: (a) discretization steps in the numerical integration; (b) low probability range of the seismic hazard curve; (c) slope of the hazard curve; and (d) log standard deviation of the fragility curve. The hazard curve, shown in Figure 1, and the median capacity of $C_{50\%}$ = 3.0g, were used in all the analyses.

Discretization Steps

The accuracy of P_F, when determined by the numerical integration, is dependent on the number of integration points. This study examines the number of integration steps needed to estimate of P_F. The discretization step (N) was varied from 6 to 120. The discretization steps cover the entire range of hazard curve 10E-3 to 10E-9, with an equal number of points in each tenfold interval (e.g., 1.0E-3 to 1.0E-4) on the hazard exceedance probability. The fragility parameters of $C_{50\%}$ = 3.0g and β = 0.4 were used in this analysis. The results in Table 1 show that, for the selected hazard curve and fragility curve, the numerical integration points of about 18 (or 3 points in each tenfold range in the probability of exceedance in the seismic hazard curve) yield reasonable accuracy for estimating probability of unacceptable performance. The calculations can be refined further, by using an increased number of integration points in the seismic hazard curve, with a significant contribution to P_F. Although a significant number of integration steps are not required in the example presented, the sensitivity of integration steps should be examined for accurate estimation of P_F, because P_F depends on the shape of hazard and fragility curves.

Table 1. Effects of Discretization Steps on P_F

N	P_F	Ratio = $P_{F,\,N=n}/P_{F,\,N=120}$
6	2.018e-5	0.8835
12	2.235e-5	0.9785
18	2.263E-5	0.9908
24	2.272E-5	0.9947
30	2.277E-5	0.9969
60	2.283E-5	0.9996
120	2.284E-5	1.0000

Low Probability Range of the Seismic Hazard Curve

A hazard curve should include a reasonable range of ground motion intensities for estimating the probability of unacceptable performance of an SSC. The sensitivity of the range of annual probability of exceedance, in the hazard curve, on the seismic risk of SSC ITS, is explored, using numerical integration. The hazard curve was terminated at probabilities of exceedance of 1.0E-5, 1.0E-6, 1.0E-7, 1.0E-8, and 1.0E-9. P_F for each case is shown in Table 2. The fragility curve, shown in Figure 2, is used in this analysis, and the number of integration points is N = 18. The effect of the range of annual probability of exceedance on P_F is indicated by the ratio column, which shows the ratio of P_F at the *H(SA)* to the P_F at *H(SA)*=1.0E-9. The results indicate that hazards at an exceedance level below 1.0E-7 have no significant effect on P_F. In this example, the low probability range of the hazard curve at exceedance level 1.0E-6 or 1.0E-7 approaches the values at the lower probability range of 1.0.E-9.

Table 2: Effect of Variation of Lower Boundary of Hazard Curve

Annual Probability of Exceedance of Hazard Curve, *H(SA)*	Probability of Unacceptable Performance, P_F	Ratio $P_{F,H(SA)}/P_{F,H(1.0E-9)}$
1.0E-5	1.766E-5	0.78
1.0E-6	2.186E-5[5]	0.97
1.0E-7	2.254E-5	0.99
1.0E-8	2.262E-5	1.0
1.0E-9	2.263E-5	1.0

Slope of the Hazard Curve

A closed-form solution method can be used to estimate the probability of unacceptable performance by assuming the hazard curve to be linear in a log-log scale. As seen in Eq. 3, P_F is controlled by slope parameter K_H or A_R and constant K_1. The slope parameter A_R, at any point on the hazard curve, is ratio of the ground motion corresponding to a tenfold reduction in hazard exceedance frequency. K_1 is computed by solving Eq. 2, where the hazard magnitude, SA, and hazard exceedance probability, *H(SA),* values correspond to the same tenfold range of the hazard curve. As seen in Figure 1, the slope of the hazard curve changes between each tenfold step of the exceedance probability on the hazard curve. In this section, selection of appropriate slope for reasonable estimate of annual probability of unacceptable performance, P_F, using closed-form solution method is discussed. The fragility parameters used for this analysis were $C_{50\%} = 3.0$g and $\beta = 0.4$. The estimated P_F values corresponding to the A_R, K_H, and K_1, at different hazard levels along the hazard curve, are given in Table 3. The plot of the actual hazard curve and the linear representations of the hazard curve at different segments are shown in Figure 4. Results show that as A_R varies between 2.16 (shallow) and 1.3 (steep), P_F varies between 3.28E-5 and 4.71E-3. Note that P_F, estimated by numerical integration, is 2.26E-5. In the cumulative distribution of P_F, shown in Figure 3, hazard between 1.2g and 2.7g spectral acceleration is the major contributor to the probability of unacceptable performance for the SSC, and the corresponding approximate range of annual probability of exceedance is 1.0E-4 and 1.0E-5. Within this range, the linearized hazard curve corresponding to the A_R equal to 1.6, overlaps with the hazard curve, as shown in Figure 4. In this example, the linearized hazard curve with slope $A_R = 1.6$ is appropriate for estimating P_F. At a given facility site, the hazard curve would remain the same; however, fragility curves for different components may have a wide variation. Thus, for evaluating seismic risk, the fragility of SSCs ITS needs to be examined in a similar manner for selecting appropriate slope from the hazard curve.

Table 3: Variation of P_F with Hazard Curve Slope

H(a)	SA	A_R^*	K_H	K_1	P_F
1.0E-3	0.753	–	–	–	–
1.0E-4	1.627	2.17	2.99	4.28E-4	3.28E-5
1.0E-5	2.603	1.6	4.90	1.09E-3	3.40E-5
1.0E-6	3.627	1.4	6.94	7.65E-3	1.76E-4
1.0E-7	4.663	1.3	9.16	1.34E-1	4.71E-3

$^*A_R = SA_{0.1H(a)}/SA_{H(a)}$, where a is spectral acceleration.

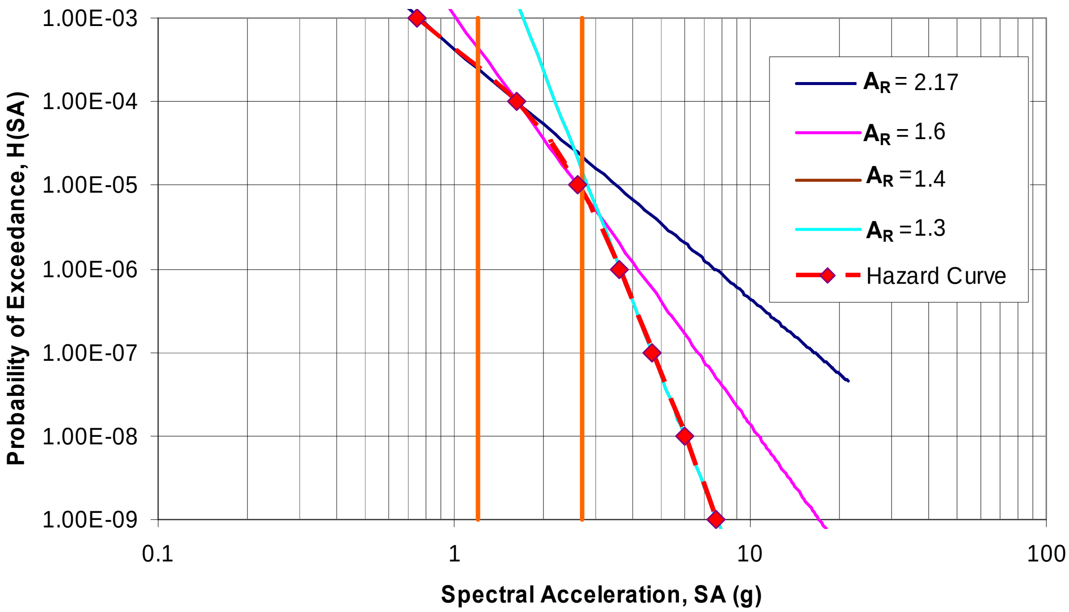

Figure 4: Hazard Curve and the linearized forms of the Hazard Curve

Log Standard Deviation

The mean fragility curve of an SSC for a selected mode of failure or limit state is typically defined as being lognormally distributed and is expressed in terms of a median capacity level, $C_{50\%}$, and a composite logarithmic standard deviation, β [2]. This section explores the sensitivity of P_F caused by variation in β.

The median capacity, β, for an SSC, can be estimated using Monte Carlo simulation, considering the variability and uncertainty of the contributing parameters. This method estimates the median capacity and the dispersion. Kennedy [6] suggested a hybrid methodology to obtain P_F. In this approach, the fragility curve is based on capacity at 1% probability, $C_{1\%}$, and an assumed value of β. The median capacity, $C_{50\%}$, can be obtained from Eq. 4. The $C_{1\%}$ point on the fragility curve is approximately equal to the High-Confidence-Low-Probability-of-Failure capacity, which is computed using a Conservative-Deterministic-Failure-Margin (CDFM) method [4] such that $C_{1\%} \approx C_{CDFM}$. The CDFM approach does not render estimate of uncertainty. The composite log standard deviation, β in Eq. 4, is independently assigned, based on judgment or past experience. ASCE 43-05 [2] recommends range of β is from 0.3 to 0.5 for structures and passive mechanical components mounted on ground, and from 0.4 to 0.6 for active components mounted at higher elevation in structures.

$$C_{50\%} = C_{1\%} e^{2.326\beta} \tag{4}$$

In this parametric study, the influence of β on P_F was examined considering fragility curves, based on $C_{50\%}$ and $C_{1\%}$ capacities. The log standard deviation β was varied from 0.3 to 0.8, as discussed earlier, to study the effects beyond the ranges suggested by ASCE [2]. Figure 5 (a) shows a plot of several fragility curves with $C_{50\%}$ = 3.0g and for different values of β. Convolving the fragility curves with the hazard curve in Figure 1 by numerical integration, the variation of P_F with β is shown in Figure 5(b). The relative increase of P_F, for different values of β, with respect to β = 0.3, is given in Table 4. As expected, the results show the mean probability of unacceptable performance increases with increasing composite uncertainty, β. The estimated values of P_F for β, ranging from 0.4 to 0.6, are about 2 to 5 times that at β = 0.3. For the highest evaluated β value of 0.8, P_F increases by about an order of magnitude. Figure 5(b) shows that P_F increases sharply beyond β = 0.5.

Fragility curves for assumed $C_{1\%}$ = 1.0g and β ranging from 0.3 to 0.8 are shown in Figure 6. The median capacity $C_{50\%}$, computed using Eq. 4, increases with composite uncertainty β, as shown in Table 5. The median capacity varies from 2.0 to 6.4g and the fragility curve anchored at $C_{1\%}$=1.0g shifts toward the right. As shown in Table 5, computed seismic risk for β ranging from 0.4 to 0.8 is about one-half to one-fourth, with respect to β = 0.3. The sensitivity of P_F to variation of β is not significant. However, contrary to the results using the $C_{50\%}$ capacity-based fragility curve, the results for this analysis, in

Table 5, show that P_F decreases with increasing β. This analysis implies that appropriate variability and uncertainty in parameters for estimating the $C_{1\%}$ capacity of the SSCs should be considered.

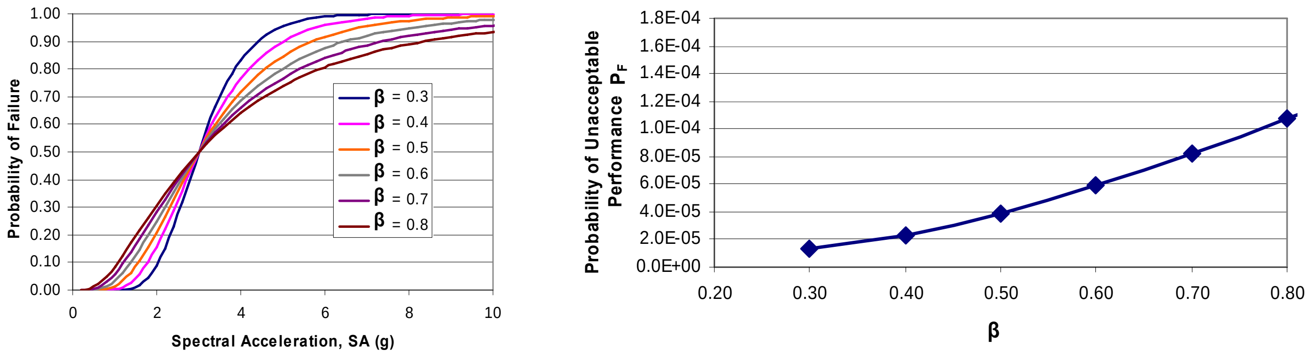

(a) (b)

Figure 5: (a) Fragility curves defined by $C_{50\%}$=3.0g and β varies from 0.3-0.8; (b) Effect of β on P_F

Table 4: Values of P_F with Varying β for $C_{50\%}$=3.0g

β	P_F	Ratio $P_{F,(\beta)}/P_{F,(\beta=0.3)}$
0.3	1.29E-05	1.0
0.4	2.28E-05	1.8
0.5	3.82E-05	3.0
0.6	5.87E-05	4.6
0.7	8.24E-05	6.4
0.8	1.07E-04	8.3

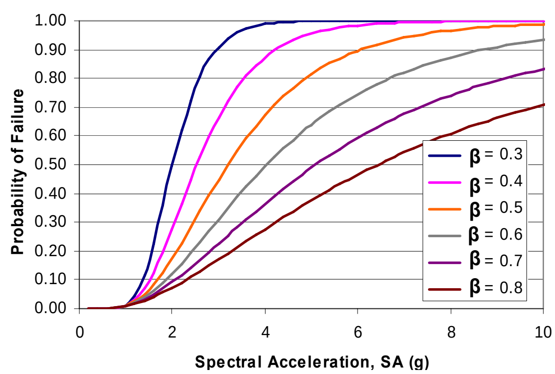

Figure 6: Fragility curves defined by $C_{1\%}$=1.0g and β varies from 0.3-0.8

Table 5: Values of P_F with Varying β for $C_{1\%}$=1.0g

β	$C_{50\%}$	P_F	Ratio $P_{F,(\beta)}/P_{F,(\beta=0.3)}$
0.30	2.01	6.85E-05	1.00
0.40	2.54	4.32E-05	0.63
0.50	3.20	3.06E-05	0.45
0.60	4.04	2.38E-05	0.35
0.70	5.09	1.99E-05	0.29
0.80	6.43	1.75E-05	0.25

CONCLUSIONS

Based on the sensitivity studies on various parameters affecting performance of SSCs and seismic risk, the following observations, limited to the parameters selected, can be made:

(1) In the numerical integration method for determining probability of unacceptable performance of SSCs, a limited number of integration steps (approximately 18 points) on the hazard curve provided reasonable accuracy in the example presented.

(2) In the numerical integration method for determining probability of unacceptable performance of SSCs, contribution of the seismic hazard curve beyond 10E-7 is negligible for this study.

(3) For the closed-form solution method for determining probability of unacceptable performance of SSCs, the use of slope of the seismic hazard curve between 1.0E-4 and 1.0E-5, yields performance results comparable to the numerical integration method.

(4) Probability of unacceptable performance of SSCs increases with increase in log standard deviation, β, for the case when the fragility curve is based on the median capacity. However, when the fragility curve of SSC ITS is based on a capacity at 1 percent on the fragility curve, the probability of unacceptable performance of SSCs decreases, with an increase in logarithmic standard deviation, β.

ACKNOWLEDGMENTS

This paper was prepared to describe work performed by the Center for Nuclear Waste Regulatory Analyses (CNWRA) for the U.S. Nuclear Regulatory Commission (NRC) under Contract No. NRC–02–02–012. The activities reported here were performed on behalf of the NRC Office of Nuclear Material Safety and Safeguards, Division of High-Level Waste Repository Safety. This paper is an independent product of the CNWRA and does not necessarily reflect the view, nor regulatory position of NRC. The NRC staff views expressed herein are preliminary and do not constitute a final judgment, nor determination of the matters addressed, nor of the acceptability of a license application for a geologic repository at Yucca Mountain.

REFERENCES

1. U.S. Nuclear Regulatory Commission, *Disposal of High-Level Nuclear Radioactive Wastes in a Proposed Geologic Repository at Yucca Mountain*, *Nevada*, Final Rule, *Federal Register*, Washington, DC, Vol. 66, No. 213, November 2, 2001, pp. 55732-55816.

2. American Society of Civil Engineers (ASCE)/Structural Engineering Institute (SEI), *Seismic Design Criteria for Structures, Systems, and Components in Nuclear Facilities*, ASCE/SEI 43-05, Reston, Virginia, 2005.

3. Electric Power Research Institute, *Methodology forDeveloping Seismic Fragilities,* EPRI TR-103959, June 1994.

4. Shah, M., *Preclosure Safety Analysis for Seismically Initiated Event Sequences,* International Symposium on *Safety Case for Deep Disposal of Radioactive Waste: Where Do We Stand?*, Organization of Economic Cooperation and Development/Nuclear Energy Agency (OECD/NEA), January 23-25, 2007, Paris, France.

5. Kennedy, R.P, *Risk-Based Seismic Design Criteria*, Nuclear Engineering and Design, Vol. 192, 1999, pp. 117-135.

6. Kennedy, R.P., *Overview of Methods for Seismic PRA and Margin Analysis, Including Recent Innovations*, OECD/NEA, Workshop on Seismic Risk , Tokyo, Japan, 10-12 August 1999.

7. McGuire, R., *Seismic Hazard and Risk Analysis*, Earthquake Engineering Research Institute, Oakland, California, 2004.

8. Kennedy, R.P. and Short, S.A. *Basis for Seismic Provisions of DOE STD-1020*, UCRL-CR-111478, U.S. Department of Energy, Washington, DC, 1994.

9. U.S. Geological Survey's website http://earthquake.usgs.gov/research/hazmaps/.

10. Park, Y. J., Hofmayer, C.H., and Chokshi, N.C., *Survey of Seismic Fragilities used in PRA studies of Nuclear Power plants*, Reliability and Systems Safety, 62, 1998, pp. 183-195.